Processing Tank Flow Mechanics for Next Generation Glass Core Substrates

Vladimir Kudriavtsev, Rajeev Bajaj, Chris Lane, Zia Karim

YES
3178 Laurelview Ct.,
Fremont, CA, 94538 USA
Ph: 1-510-954-6889
Email: zkarim@yieldengineering.com, zkarim@yes.tech

Abstract
Glass substrates are increasingly seen as an alternative for interposers in heterogeneous packaging [1]. In a typical wet tool, substrates undergo chemical treatments in separate tanks. Standard panels (510x515mm) are processed simultaneously, requiring a carrier for automated loading, unloading, locking, and transportation. This study examines flow velocities between panels, carrier walls, and tank walls in stationary positions. The overflow tank, a crucial sparger system component, has three fluid parts: the lower distribution area, a separation plate, and the main tank. To enhance the design, we study the interplay between porous resistances, showerhead coverage, carrier-to-platform distance, carrier-to-free surface distance, carrier-to-wall gaps, and distances between panels. Our approach aims for a custom flow field in the sparger tank that is as uniform and unidirectional as possible. Designing tank and carrier components to prevent stagnation zones ensures shorter residence times, critical for the sparger system's effectiveness. Our findings apply to wet chemical etching of TGV vias or electroless metal (Ni, Cu, etc.) deposition processes.

Key words
Glass interposer, sparger tank, wet processing, TGV etch, electroless deposition, flow uniformity, CFD

I. Introduction
Experts in the industry view glass substrates as a promising alternative material for interposers, particularly in heterogeneous packaging such as 2.5D or 3D packages [1]. Recently, Intel revealed that they have developed one of the industry's first substrates specifically tailored for advanced packaging of the next generation [2,3]. Using Through-Glass Vias (TGV) on glass panels is a crucial technique for creating 2.5D/3D packaging solutions [4]. Glass substrates offer advantages such as rigidity, flatness, and thermal stability, enabling a tenfold increase in interconnect density. This is combined with high resistivity, low dielectric constant, low insertion loss, adjustable coefficient of thermal expansion and lower cost.

To create via holes, laser techniques are initially used [4,5], followed by wet etching to achieve the proper diameter. Then, metal and thin-layer depositions are carried out through various methods, including electroless plating, electroplating, PVD, and CVD. This paper focuses on optimizing wet tank processes to achieve the best planar uniformity during the wet processing step.

A typical wet tool for processing glass panels involves multiple steps, with each step taking place in a separate tank. The substrates are immersed in different chemical solutions one after the other in a consecutive linear fashion. The process must maintain uniformity so that deposition or etching occurs similarly at various parts of the panel. The standard size of the panel is 510x515mm, and multiple glass substrates are usually processed simultaneously. Therefore, a panel carrier must be designed for successful high-volume manufacturing. This carrier should allow for practical automated loading and unloading of panels, absorbing loads, and withstanding hydraulic impacts, as well as locking panels and transporting the carrier between various tanks.

When a carrier containing multiple panels, locking pads, and mechanisms are lowered inside a tank, it can remain stationary or move up and down or side to side, enhancing mixing. Bubbles can also be introduced for the same purpose, creating a more effective mixing process.

TGV vias and similar features require special attention as precursor chemicals need to enter a ~50-micron-sized via and then diffuse or convect in and out while removing byproducts. In this study, we analyze planar phenomena and micron-sized processes separately or by incorporating embedded links. We also focus on fluid dynamics and correlate velocity distributions with actual process measurements.

II. Tank Setup

While pilot production lines, as shown in [1-3], may process a single panel in a single tank (Figure 1) for design optimization purposes, we have to consider the interplay between the rather complex carrier geometry, multiple panels, including locking pads and related mechanisms, and the rest of the tank volume.

Two different types of sparger tanks exist [7]: the Piping-Sprayer (PS) and the Perforated-Plate-Sprayer (PPS). Yield Engineering, continuing with the legacy of SPEC (Valencia), develops systems based on the PPS principle. It was shown in [7] that such a system provides superior uniformity and flow control compared to PS systems and, if properly designed, can achieve exceptional performance.

A typical configuration is shown in Figure 2. The carrier can move up and down between two characteristic positions. For each reference position, key design parameters include the distance between the bottom of the tank and the bottom of the carrier, the distance between the top of the carrier and the weir edge, four gaps between the carrier and the walls, tank dimensions (HxWxL), various offset distances between the panel and carrier inner walls, pitch between the panels, mounting pad placements, and dimensions.

The overflow tank comprises three primary fluid components: the lower distribution area, porous separation plate, and the main tank where the carrier and panels are located. The lower distribution area has a higher velocity turbulent flow, while the PPS-type distribution can be designed and patterned differently depending on the application. Lower tank dimensions and the number of pipe inlets determine the shapes of recirculations, which are linked with the planar inlet uniformity of the showerhead. Usually, the higher the flow resistance of the perforated plate, the less hydraulic coupling between the two tanks, and higher overall planar uniformity. One can study these tanks separately; however, it was shown in [8] that these processes are highly coupled, so we study them in a fully coupled manner.

Figure 1. Glass panel Lowered into Wet Processing overflow tank in a pilot line [1]

The overflow tank is a crucial component of the sprager system, and it usually has a capacity of 150-300 liters. The tank undergoes 4-10 complete volume changes every hour. The mass flow rate typically ranges between 30-80 liters per minute, resulting in average velocities of 3-5 mm/s. These flowrates ensure a uniform distribution of flows. Between the panels, while this can not be maintained in larger open volumes in the tank, especially its lower distribution zone.

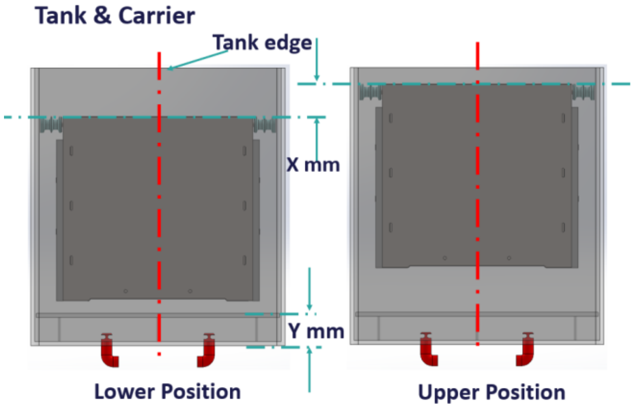

Figure 2. Carrier inside the tank- characteristic positions

Our design approach estimates the velocity flow field (U, V, P) in the sparger tank to be as uniform and unidirectional as possible, particularly in the areas between the panels. We design the individual tank and carrier components to avoid the formation of stagnation zones or zones with backflow. This design ensures shorter residence times, which are critical for the effectiveness of the sprayer system. The convective process leads to boundary layer formation, while diffusion across the boundary layer determines the access of fresh precursors to the surface. Therefore, our findings apply equally to wet surface reaction-driven processes, such as alkaline chemical etching of TGV glass vias (using NaOH, KOH [9]) or Ni, Cu electroless processes [11,12].

III. CFD Study: Model

In the design exploration study, we aim to optimally select key design variables, such as carrier and tank dimensions and then proceed with the optimization of individual design variables. Parametric CAD models are created in SolidWorks and used to generate Computational Fluid Dynamics (CFD) numerical setups, either in addition to or instead of an experimental flow visualization tank. This study examines the flow velocities between the panels, the carrier walls, and the tank walls in stationary up and down positions. The flow field is obtained by numerically integrating the incompressible Navier-Stokes equations using software packages like ANSYS CFX, FLUENT, Discovery, and COMSOL for computational fluid dynamics (CFD). Both different flow options are considered. The model utilizes half-tank symmetry, as illustrated in Figures 4A-C. Mass flow or fixed velocity is specified at the pipe inlet in the bottom tank, the free surface uses a zero shear (slip) boundary condition, pressure outlet boundary conditions are applied above the edge of the tank, and symmetry boundary conditions are set at the half-tank plane.

The typical process flow involves the computational finite volume or finite-element volume mesh representation of the liquid volume when solid parts are suppressed, and intricate spaces between various elements are filled with watertight volumes, facilitating the solution process. The solution involves solving systems of linear algebraic equations where mass flow and momentum balances are written in each elementary mesh element (volume) and solved by a matrix solver. Due to the tank's complexity, the typical model includes 3-10 million elements and requires hours or days of CPU time on parallel clusters and Nvidia Quadro5000 GPU.

Flow resistance in the perforated plate is calculated using the Darcy-Forchheimer approximation,

$$\Delta P = \frac{\mu}{K} \cdot U + \frac{\rho}{K_f} \cdot U^2$$

ΔP is the pressure drop,

μ is the dynamic viscosity of the fluid,

K is the permeability of the porous medium,

U is the velocity of the fluid flow,

ρ is the fluid density, and

K_f is the Forchheimer coefficient.

Coefficients (K and K*f*) are obtained separately by directly solving the flow through a smaller segment of orifices, as shown in Figures 3(A, B). Typical examples of Forchheimer coefficients are presented in Table 1 below.

	K	**K*f***
Design A	1.17e-8	16, 752
Design B	3. 3e-8	16, 180
Design C	2.83e-9	178,309

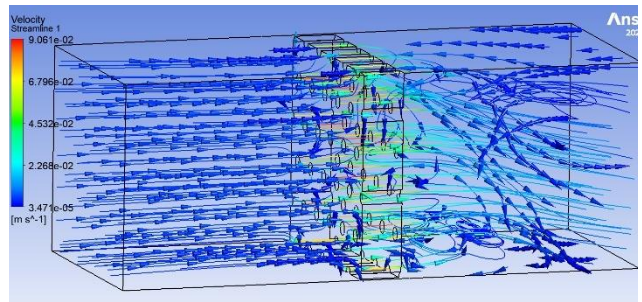

Figure 3A. Reference model to determine flow resistance of the Perforated plate (porous media)

To achieve an optimal design trade-off, we study the interplay between porous resistances, perforated plate planar coverage, carrier-to-platform distance, carrier-to-free surface distance, carrier-to-wall gaps, and distances between individual panels.

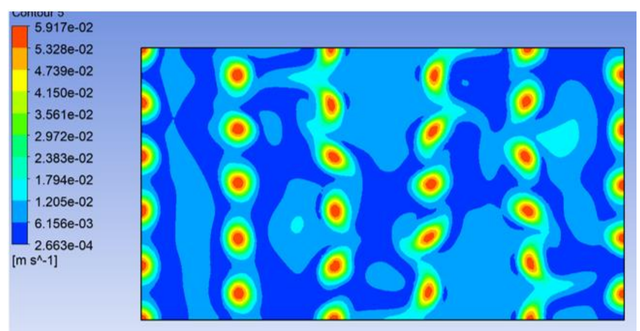

Figure 3B. Velocity map of jets passing perforated plate shown in Figure 3A. Notice how uniform velocity magnitudes are.

Our approach involves creating a custom flow field in the sparger tank that is as uniform and unidirectional as possible, particularly in the areas between the panels. We carefully design the individual tank and carrier components to prevent the formation of stagnation zones or backflow, ensuring shorter residence times within the system, which are crucial for the effectiveness of the sparger system. This focus on design promotes better fluid dynamics and chemical transport throughout the system, enhancing process efficiency. Our preference is for uniform velocity everywhere, between the panels and also outside the panels, in areas next to side walls, for example. However, designers face numerous dilemmas related to fitting the carrier that contains the panels, aligning carrier transport with the tank, and accommodating various parts required for carrier operation, such as shakers and lifters. Therefore, the main objective is ensuring uniform flow between the panels, with secondary priority given to uniformity elsewhere.

The convective process plays a dominant role in chemical transport within the boundary layer of the system, impacting fluid flow dynamics and chemical reactions. Our design principles are equally applicable to a wide range of processes, including wet chemical etching of TGV vias using substances like NaOH or electroless processes involving metals like Ni and Cu. Prioritizing the prevention of stagnation zones and backflow ensures that fluid flow remains optimized, leading to consistent and reliable outcomes in manufacturing processes.

IV. CFD Study: Results

In Figure 4A, we demonstrate an example of the flow visualization of the overflow tank-carrier-perforated plate and lower tank (with multiple inlet pipes) system. We use streamlines to highlight general flow directions in various parts of the tank, which are also colored by velocity to indicate areas of crowding (higher velocity). The lower tank below the perforated plate shows butterfly-like flow formations, depicted in greater detail in Figure 4B. Multiple horizontal cross-sections highlight in-plane uniformity and redistribution of mass flow as it rises from the bottom of the tank towards the free surface. Additionally, we demonstrate flow uniformity on the free surface, and velocity streamlines point to tank edges, showing no backflow or recirculatory motion that can keep particles afloat at the liquid-gas interface for prolonged periods.

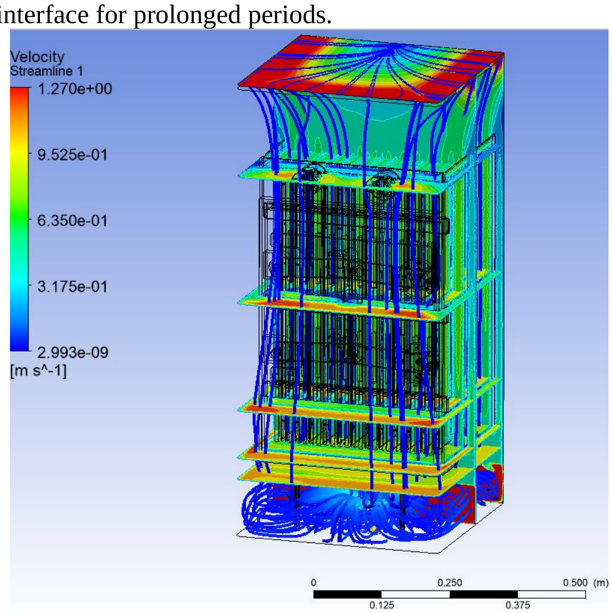

Figure 4A Example of Carrier-Tank Flow Visualization, half tank is shown

Several vertical cross-sections are also included to demonstrate in-plane velocity distribution, such as at the tank planes of symmetry placed at their width and length dimensions.

As seen in Figures 4(B-C), while flow recirculations in the lower tank are complex and significant due to the high flow rate, properly selected resistance of the perforated plate results in uniform vertical streamlines, indicating that both tanks are largely decoupled and achieving the required objective.

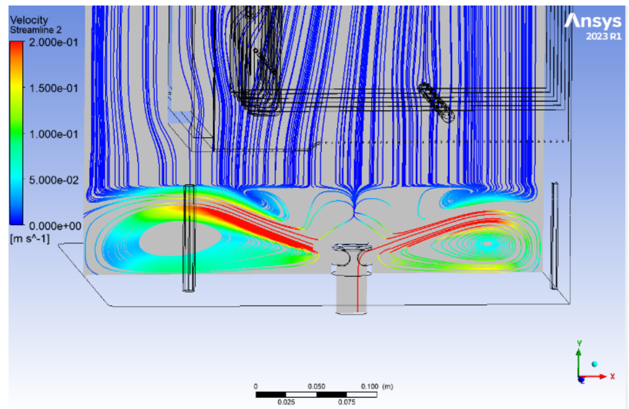

Figure 4B. Lower Tank Flow Detail

In Figure 4C, we highlight the complex mixing nature as fluid flow exits the distribution pipe, with a symmetry plane on the right-hand side. This accounts for two pipes in the full tank geometry, with jets coming from these pipes at high velocity colliding and interacting with each other.

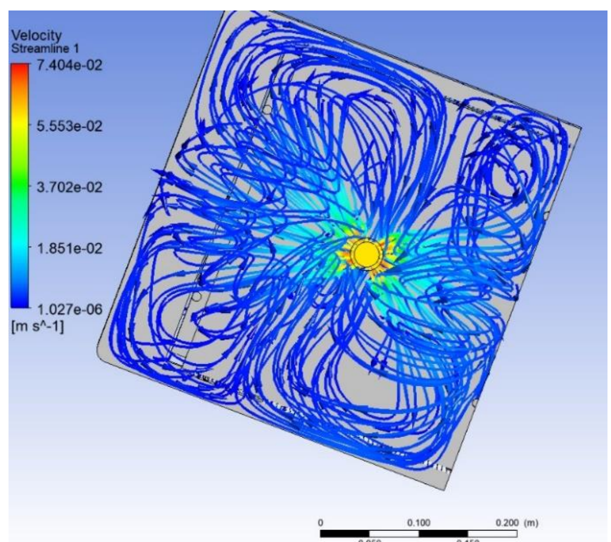

Figure 4C. 3D Streamlines in the lower tank

Figure 5A displays flow streamlines passing through a wider cross-section of the tank, emphasizing their straightness and the straight and unidirectional flow within the tank with panels. The wireframe in the background highlights the complex carrier parts and mounting features.

Figure 5C demonstrates velocity maps in the same plane as Figure 5A and in the plane perpendicular to the one shown in Figures 5B and 5D.

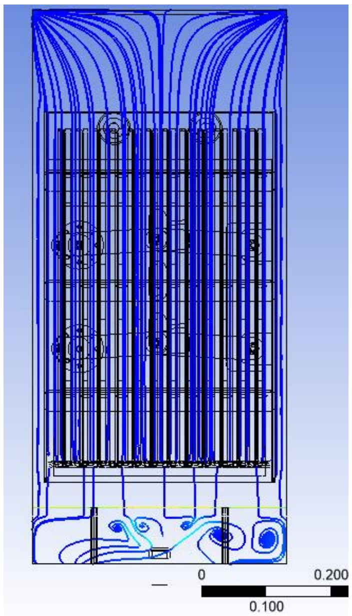

Figure 5A Vertical Cross-section, streamlines

While flow in the gap between the carrier and tank wall has lower velocity, velocity between all panels is very uniform (red color) across the entire stack. The same is true for the velocity map in the perpendicular plane, as shown in Figure 5D. Streamlines are straight, and key areas inside the carrier have the same velocity (green color on the figure).

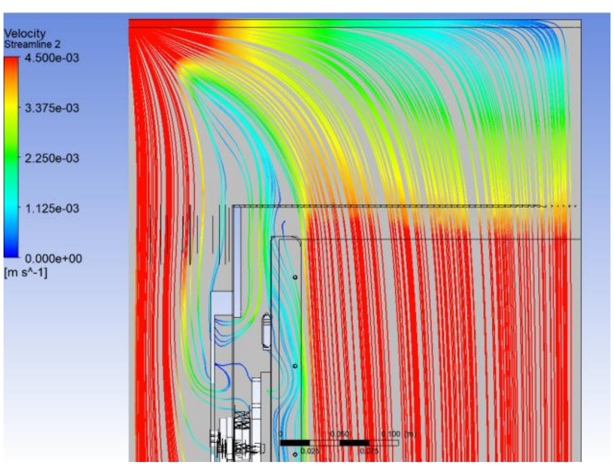

Figure 5B. Vertical Cross-section Streamline Detail

This stack consists of 12 panels and added carrier walls, with a laminar boundary layer formed between the panels, depicted by the blue color (indicating low velocity) since the velocity component on the wall is equal to zero.

Both Figures 5B and D show a significant zone occupied by mechanisms where flow is slower, which is physically and mechanically unavoidable. However, we can see from the presented results that these areas are clearly localized.
The vertical velocity component (W=0) at the free surface forces flow to turn around, naturally creating a zone of lower velocity in the center of the tank. In the presented design, the flow above panels has plenty of space to turn around, and interface proximity does not negatively affect uniformity.

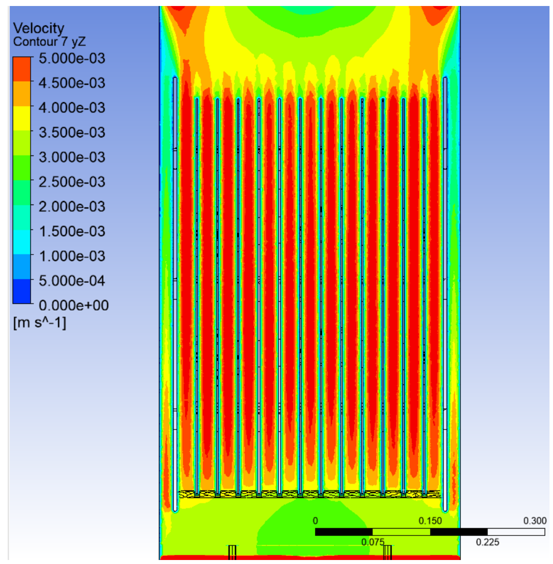

Figure 5C. Vertical Cross-section Velocity Map

In Figure 5d, the lower tank (below the perforated plate) is shown in red color, indicating much higher jet velocities in that area. However, as the jets pass through the perforated plate (segment shown in Figures 3A-B), their velocity is averaged to much lower values and becomes uniform across the cross-section shown.

The higher velocity zone on top of the tank (Figure 5C) is formed due to the natural need for the flow to exit through a much smaller cross-section that forms over the edge of the tank, typically not exceeding 7-8mm for our flow rates. According to Bernoulli's Law, velocity needs to increase in such cases. This increase in velocity can lead to potentially higher velocity flows in the gap between the carrier and the tank, as well as in the gaps between the panels that are adjacent to those gaps. Figures 6A and 6B show multiple in-plane horizontal velocity maps. In both figures, the plane of tank symmetry is on the right-hand side. In this simulation, data from Table 1

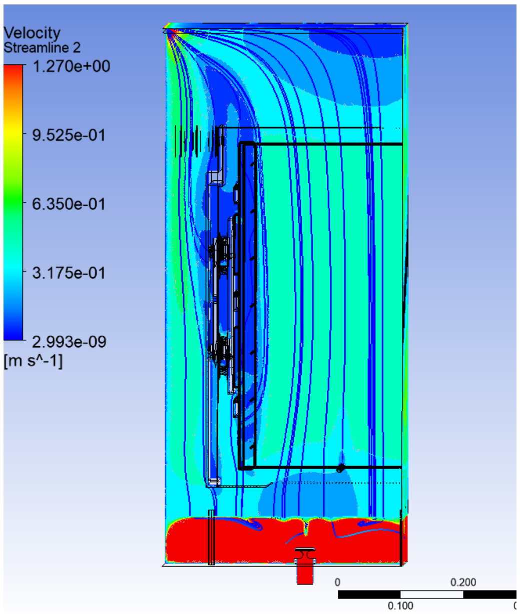

Figure 5D. Middle Between Panels Cross-section

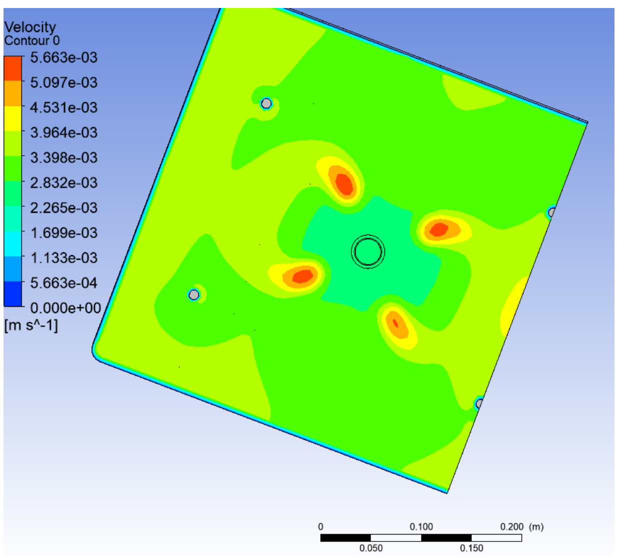

Figure 6A. Perforated Plate in Plane Velocity Map

was utilized, matching one of YES's proprietary designs. Figure 6A shows the vertical velocity contour, where we notice that velocity does vary but in a very uniform fashion, (~15% variation) dominated by green color. Jets leaving the distribution pipe result in small zones of higher velocity (red spots). The horizontal in-plane velocity contours shown in Figure 6B illustrate a zone of higher velocity between the carrier and the tank wall, with 4 cross-sections displayed. This area can be further optimized, however, it is necessary to facilitate due to carrier handling requirements. These areas are outside of the panel processing zone. Cross-section number 3 from the bottom shows contour interruptions, quite visibly. These are due to the support bar placement shown on plane number 2. This is the wake "imprint" behind the support bar, also shown in the perpendicular plane (as the yellow triangle) in Figure 7.

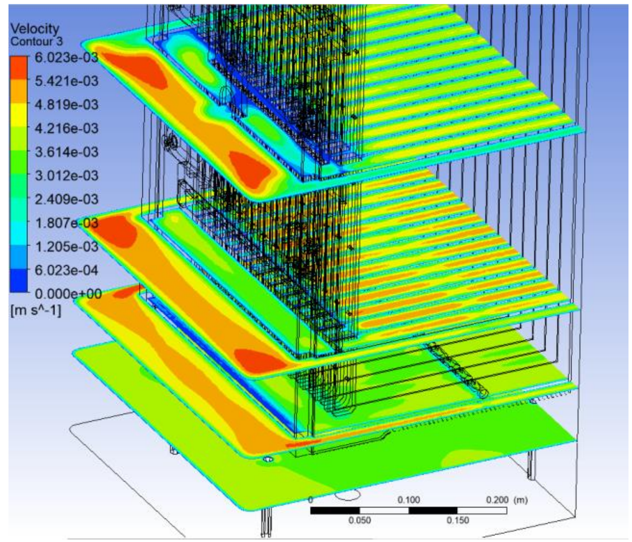

Figure 6B. Example of horizontal cross-section in the middle of the tank

Similar to the results highlighted in Figures 5B-D, we can find in Figure 7 that while velocity stagnation in the area occupied by mechanical parts (blue color) is significant, at or near panel edges, streamlines are straight, and the velocity field is uniform. From Figure 7, we can see that the wake zone extends up to 20% of the panel's vertical length, and further flow optimization of the bar and reduction of its cross-section will be needed to diminish this effect. This can also be achieved by flow bubbles, typically utilized in most tank designs.

An example of poor design is depicted in Figure 8. We can observe significant lateral deflections of the flow lines, resulting in the formation of leading-edge recirculation, which can cause an aircraft stall in aviation. In this context, these deflections block the inflow between the panels, reducing flow velocity and ultimately leading to backflow.

V. Conclusions

This study presents a method for fluid design in advanced tanks used for processing glass interposer panels. The method allows for both the design of a better functional system and the visualization and understanding of complex interplays and relationships in nonlinear fluid phenomena. The method employs computational fluid dynamics (CFD) to solve the Navier-Stokes equations for incompressible flow, implemented using commercial software packages such as ANSYS CFX, FLUENT, and COMSOL, all of which were utilized in this work. We discuss the approach to achieving flow uniformity, highlighting the differences between traditional sparger pipe designs and the perforated plate design we employ. The example design analyzed

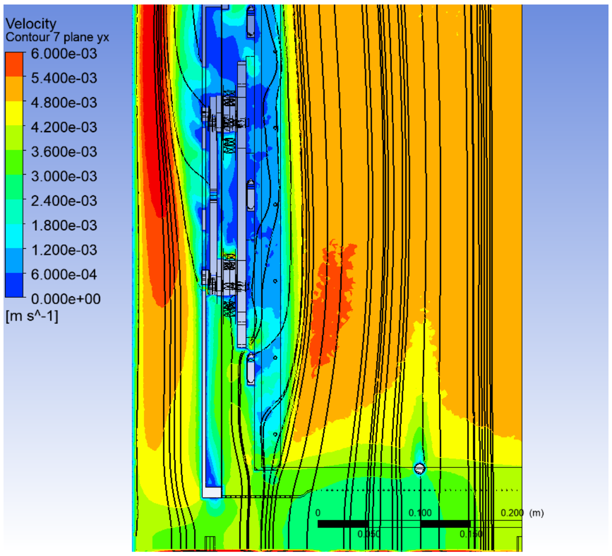

Figure 7 Effect of Structural Elements, horizontal bars on the flow field

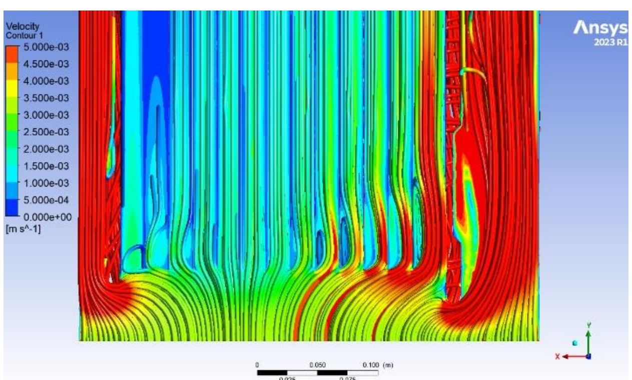

Figure 8. Example of poor tank flow design

in this paper features perforated plate distribution at the bottom of the tank, offering inherent advantages in uniformity, adjustability, and modularity required for high-volume production. The authors conducted a range of parametric studies for the baseline geometry considered, for example studying the effect of the gap between the panels. However, those studies are outside the scope of this paper. Future studies will integrate surface etching and electrochemical reactions into the computational models [9,11]. For example, the rate constant for the reaction of glass fiber with alkaline solution at 95 °C was found to be between 1.3×10^{-4} and 4.3×10^{-4} g/(m² s). The reaction order (n) was determined as 0.31–0.49 with respect to the alkaline solution, and the activation energy was 58–79 kJ/mol [9]. This way, not only velocity but also species concentrations and surface etch or deposition rates can be mapped on the surfaces of panels.

.

Acknowledgement

The authors would like to acknowledge the help of design engineers who put this complex model together to enable this study, namely John Babin, Aleksey Khrustalev, and Terry Peterson. Appreciation also goes to the YES Process Engineering team, Hratch Mouradian, Sossan Wali, Cobe Tao, and Venu Govindarajulu for useful discussions.

References

[1] *What is a Glass substrate? – a game changer of semiconductor packaging! https://www.youtube.com/watch?v=RZDlZmaxClw*W.-K. Chen, *Linear Networks and Systems* (Book style). Belmont, CA: Wadsworth, 1993, pp. 123–135.

[2] *Babak Sabi, Intel senior vice president and general manager of Assembly and Test Development, Glass Substrates explained in 60seconds, https://www.intel.com/content/www/us/en/newsroom/news/intel-unveils-industry-leading-glass-substrates.html#gs.4kwmb5*.

[3] Intel advanced packaging with Glass Substrates, https://www.youtube.com/watch?v=i4OwIQcM60o

[4] Lucas A. Hof, Zana Abu Ziki, Micro hole drilling in glass substrates-review, Micromachines, Micromachines *2017,* 8*(2), 53; https://doi.org/10.3390/mi8020053, p.1-23*

[5] J. Kim, S. Kim, B. Kim, J. Choi, S.Ahn, Study of Through Glass Vias and selective chemical etching, Micromachines, 2023, 14, 1776

[6] Lena Mohr, M. Zimmer, A. Moldovan, M. Menschik, B. Mandlmeie, C. Muller, Fluid Dynamic Modeling of an Industrial Chemical Process Bath for the Production of Silicon Solar Cells, Proceedings of the 2017 COMSOL Conference, Rotterdam, pp1-7

[7] Mohd Omar Mukhtar Zainul Azmi1, Kahar Osman1, Nor Azwadi Che Sidik2, Muhammad Noor Afiq Witri, Muhammad Yazid and Mohamad Ikhwan Kori, Computational Fluid Dynamics Analysis of Sparger Systems in Electroless Nickel Plating Processing Tank Journal of Tomography System & Sensors Application Vol.2, Issue 2, ISEMT 2019

[8] I. E. Idelchik, Norman A. Decker, Mark Steinberg , Fluid Dynamics of Industrial Equipment: Flow Distribution Design Methods, 1st Edition, CRC Press, May 1991, 403p

[9] Sairah Bashir, Liu Yang,J. J. Liggat Jim Thomason, Kinetics of dissolution of glass fibre in hot alkaline solution, Journal of Materials Science 53(5), Feb. 2018, DOI: 10.1007/s10853-017-1627-z

[10] S. Bamberg, M.Merschy, T. Bernhard, F. Bruening Challenges of Adhesion Promotion for the Metallization of Glass Interposers, Atotech, 46th International Symposium on Microelectronics, IMAPS 2013, Orlando, FL

[11] Karan Pawar, Pradeep Dixit, A critical review of copper electroless deposition on glass substrates for microsystems packaging applications, pages 576-617, Published online: 08 Nov 2022, https://doi.org/10.1080/02670844.2022.2142002, Surface Engineering, Vol. 38, 2022 -Issue 6

[12] Swatilekha Ghosh, Electroless copper deposition: A critical review, Thin Solid Films, Volume 669, 1 January 2019, Pages 641-658 https://doi.org/10.1016/j.tsf.2018.11.016